

Amorphous/Crystalline Hetero-Phase Pd Nanosheets: One-Pot Synthesis and Highly Selective Hydrogenation Reaction

Nailiang Yang, Hongfei Cheng, Xiaozhi Liu, Qinbai Yun, Ye Chen, Bing Li, Bo Chen, Zhicheng Zhang, Xiaoping Chen, Qipeng Lu, Jingtao Huang, Ying Huang, Yun Zong, Yanhui Yang, Lin Gu, and Hua Zhang*

Similar to heterostructures composed of different materials, possessing unique properties due to the synergistic effect between different components, the crystal-phase heterostructures, one variety of hetero-phase structures, composed of different crystal phases in monometallic nanomaterials are herein developed, in order to explore crystal-phase-based applications. As novel hetero-phase structures, amorphous/crystalline heterostructures are highly desired, since they often exhibit unique properties, and hold promise in various applications, but these structures have rarely been studied in noble metals. Herein, via a one-pot wet-chemical method, a series of amorphous/crystalline hetero-phase Pd nanosheets is synthesized with different crystallinities for the catalytic 4-nitrostyrene hydrogenation. The chemoselectivity and activity can be fine-tuned by controlling the crystallinity of the as-synthesized Pd nanosheets. This work might pave the way to preparing various hetero-phase nanostructures for promising applications.

different materials, which could combine the advantages of individual components and/or overcome their drawbacks.^[2] Similar to the heterostructures composed of different materials, crystal-phase heterostructure, as one kind of hetero-phase structures in monometallic nanomaterials, was proposed for the investigation of crystal-phase-based applications^[1c] and also used for the epitaxial growth of novel nanostructures for promising applications.^[3]

Different from crystals, amorphous materials might exhibit intriguing properties and applications.^[4] Inspired by the crystal-phase heterostructures, it is desired to develop a facile synthetic strategy for preparation of the amorphous/crystalline hetero-phase noble

Noble metal nanocrystals have shown various promising applications in optics, catalysis, electronics, and so on, due to their unique physiochemical properties, which strongly depend on their shape, size, exposed facet, dimension, and atomic arrangement.^[1] In order to prepare novel nanostructures with multi-functionalities and/or enhanced properties, one of the effective strategies is to synthesize heterostructures with

metal nanomaterials, which might exhibit unique properties and promising applications compared to their amorphous and crystalline counterparts. To the best of our knowledge, there is rarely report on the preparation of amorphous/crystalline hetero-phase noble metal nanomaterials, since it is quite challenging to obtain amorphous noble metal nanomaterials due to the strong metallic interactions between the atoms.^[5]


Dr. N. Yang, H. Cheng, Q. Yun, Y. Chen, Dr. B. Chen, Dr. Z. Zhang,
Dr. Q. Lu, J. Huang, Dr. Y. Huang, Prof. H. Zhang
Center for Programmable Materials
School of Materials Science and Engineering
Nanyang Technological University
50 Nanyang Avenue, Singapore 639798, Singapore
E-mail: hzhang@ntu.edu.sg

X. Liu, Prof. L. Gu
Beijing National Laboratory for Condensed Matter Physics
Institute of Physics
Chinese Academy of Sciences
Beijing 100190, China
X. Liu
School of Physical Sciences
University of Chinese Academy of Sciences
Beijing 100049, China

Dr. B. Li, Dr. Y. Zong
Institute of Materials Research and Engineering
A*STAR (Agency for Science, Technology and Research)
2 Fusionopolis Way, Innovis #08-03, Singapore 138634, Singapore

X. Chen
School of Chemical and Biomedical Engineering
Nanyang Technological University
Singapore 637459, Singapore

Dr. Y. Yang
Institute of Advanced Synthesis
School of Chemistry and Molecular Engineering
Jiangsu National Synergetic Innovation Center for Advanced Materials
Nanjing Tech University
Nanjing 211816, China
Prof. L. Gu
Collaborative Innovation Center of Quantum Matter
Beijing 100190, China

 The ORCID identification number(s) for the author(s) of this article can be found under <https://doi.org/10.1002/adma.201803234>.

DOI: 10.1002/adma.201803234

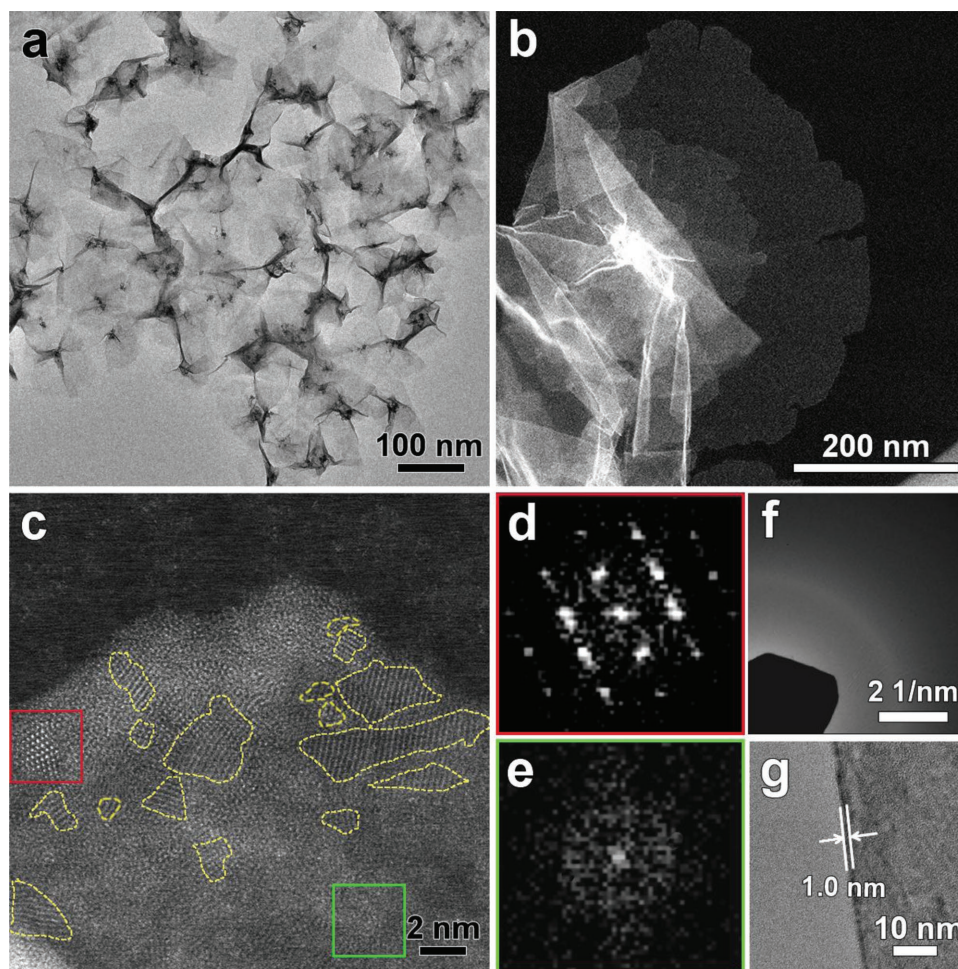


Figure 1. Characterization of the hetero-phase Pd nanosheets in Sample 1. a) TEM and b) DF-STEM images showing the nanosheet morphology. c) C_S -corrected STEM-HAADF image showing the hetero-phase structure, in which the crystalline domains are marked by the dashed yellow curves. d,e) The corresponding FFT patterns of the selected regions marked by the red and green squares, respectively, in (c). f) SAED pattern of Sample 1. g) TEM image of a folded Pd nanosheet, showing the folded edge with measured width of ≈ 1.0 nm.

Herein, by using a one-pot wet-chemical method, the amorphous/crystalline hetero-phase Pd nanosheets have been synthesized, which are then used as the catalysts for selective hydrogenation of 4-nitrostyrene. The crystallinity of hetero-phase Pd nanosheets can be controlled by fine-tuning the experimental conditions. Importantly, with proper control over the crystallinity of hetero-phase Pd nanosheets, their high catalytic activity and excellent selectivity have been achieved.

In a typical experiment, in order to prepare hetero-phase Pd nanosheets with different crystallinities, the $\text{Pd}(\text{acac})_2$ was reduced by CO, which was released by the decomposition of $\text{Mo}(\text{CO})_6$,^[6] in octanoic acid at various temperatures (48–100 °C) for 40 min (see the Supporting Information for details). The Pd nanosheets obtained at 48 °C are denoted as Sample 1 (Figure 1). Transmission electron microscopy (TEM) (Figure 1a) and dark-field scanning TEM (DF-STEM) (Figure 1b) images confirm that the nanosheets with high purity were obtained. The spherical aberration-corrected STEM-high-angle annular dark-field (C_S -corrected STEM-HAADF) image (Figure 1c) shows that a typical nanosheet is composed of crystalline and amorphous domains, which are further identified

by the bright spots (Figure 1d) and diffuse ring (Figure 1e) in the corresponding selected-area fast Fourier transform (FFT) patterns, respectively. For clarity, the crystalline domains are marked by the dashed yellow curves (Figure 1c). Moreover, the weak ring in the selected area electron diffraction (SAED) pattern (Figure 1f) further reveals their poor crystallinity. The average width of the folded edge in nanosheets was measured to be ≈ 1.0 nm (Figure 1g), which corresponds to the thickness of nanosheets,^[7] proving their ultrathin structure.

Our synthetic method is quite general. By simply tuning the synthetic temperature, a series of hetero-phase Pd nanosheets with different crystallinities, referred to as Samples 2–5, are obtained at 52, 60, 80, and 100 °C, respectively. All of the nanosheets (Figure 2a–d, Figure S1a–d, Supporting Information) possess a similar thickness of ≈ 1.0 nm, measured from the folded edges in high-resolution TEM images (Figure S1e–h, Supporting Information). It is ≈ 2.0 nm thinner than the thickness measured by atomic force microscopy (≈ 3.0 nm, Figure S2, Supporting Information), due to the octanoic acid molecules coating on the double-side surfaces of Pd nanosheets.^[8] The C_S -corrected STEM-HAADF images show

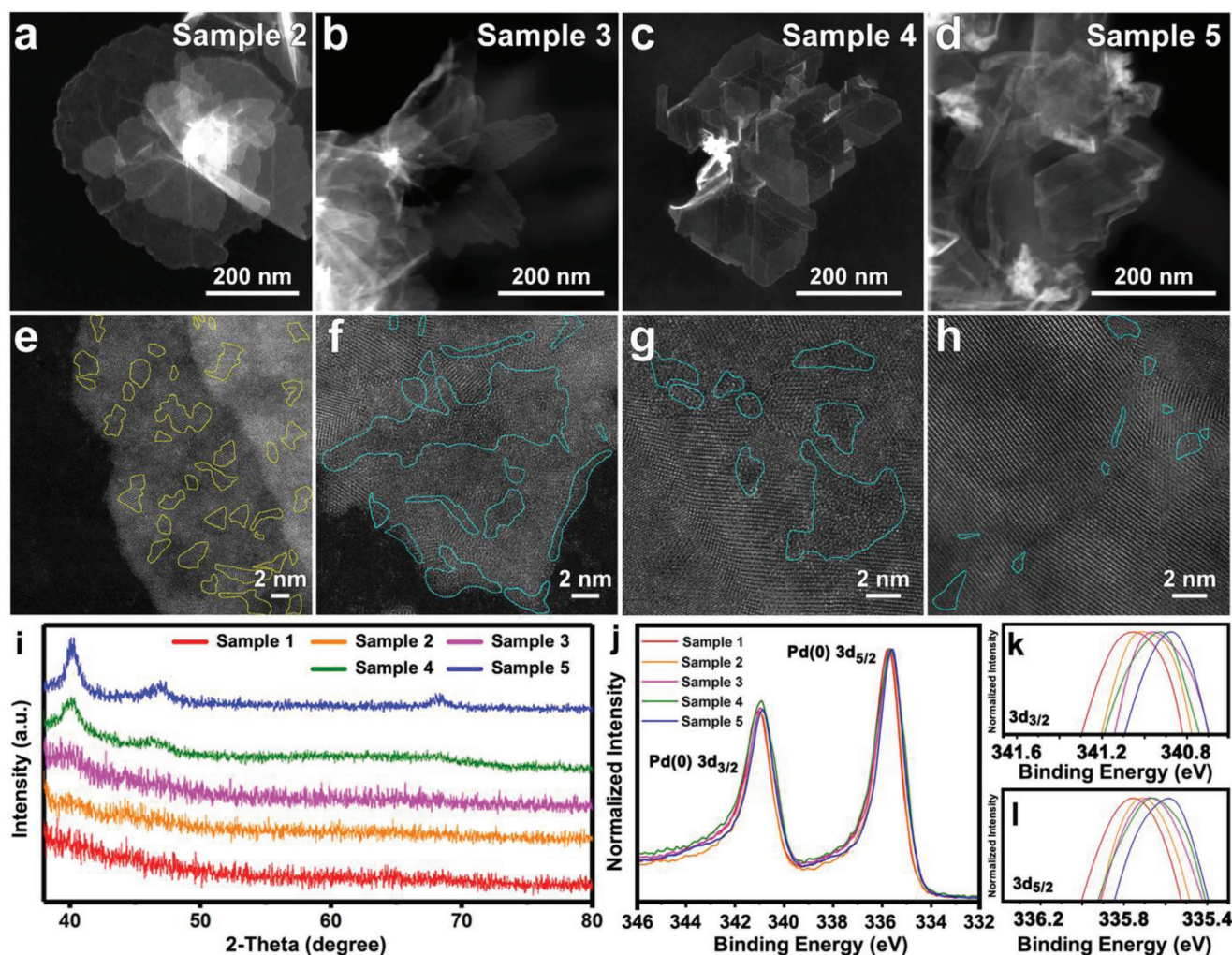


Figure 2. Characterization of the hetero-phase Pd nanosheets with different crystallinities. a–d) DF-STEM and e–h) C_s -corrected STEM-HAADF images of the hetero-phase Pd nanosheets in Samples 2–5, respectively. The crystalline domains are marked by the dashed yellow curves in (e), while the amorphous domains are marked by the dashed light-blue curves in (f–h). i) XRD spectra of Samples 1–5. j) XPS spectra of Pd 3d for Samples 1–5. k) The magnification of the normalized Pd(0) $3d_{3/2}$ peaks in Samples 1 to 5. l) The magnification of the normalized Pd(0) $3d_{5/2}$ peaks in Samples 1–5.

that these nanosheets are also composed of amorphous and crystalline domains (Figure 2e–h), and the area of amorphous domains decreases from Sample 2 to Sample 5. By measuring the areas of the amorphous and crystalline domains in the C_s -corrected STEM-HAADF images, the percentages of the crystalline areas in Samples 1–5 are estimated to be $\approx 11\%$, 19%, 65%, 83%, and 96%, respectively. Moreover, the X-ray diffraction (XRD) was used to characterize the crystallinity of the hetero-phase Pd nanosheets. As shown in Figure 2i, there is no obvious diffraction peak for Sample 1, indicating that the dominant phase of Sample 1 is amorphous, consistent with the aforementioned results (Figure 1). The intensity of diffraction peaks attributed to the face-centered cubic Pd (PDF# 46–1043) increases from Sample 1 to Sample 5 (Figure 2i), indicating the increased crystallinity, which has also been proved from the increasingly intensive diffraction rings in the SAED patterns in Samples 1–5 (Figure 1f, Figure S1i–l, Supporting Information). Furthermore, X-ray photoelectron spectroscopy (XPS) taken from Samples 1–5 was used to confirm their different electronic structures (Figure 2j–l). The Pd(0) $3d_{3/2}$ and

Pd(0) $3d_{5/2}$ peaks gradually shift to lower binding energy from Sample 1 to Sample 5. This observation, i.e., the amorphous nanosheet has a greater binding energy, is consistent with the previous report.^[9] Meanwhile, there is no signal from Pd(II), indicating the metallic state of the synthesized Pd nanosheets.

Noble metals, such as Pd, have been widely used as the heterogeneous catalysts for hydrogenation,^[10] which is very important in the industrial and fine chemical fields.^[10b,11] However, it is very challenging to achieve the highly selective hydrogenation of molecules containing both C=C double bonds and nitro groups, since both functional groups can be readily hydrogenated.^[10b,11] Herein, as a proof-of-concept application, in order to investigate the correlation between the chemoselectivity/catalytic activity and the crystallinity of noble metal catalysts, the hetero-phase Pd nanosheets are used in the hydrogenation of 4-nitrostyrene (NS), which is commonly used as the model reaction.^[10d,12] Figure 3a presents three products after the hydrogenation of NS. The selective hydrogenation of C=C bond generates the 4-nitroethylbenzene (EN), whereas the selective reduction of nitro group produces the 4-aminostyrene (AS). Finally, the fully

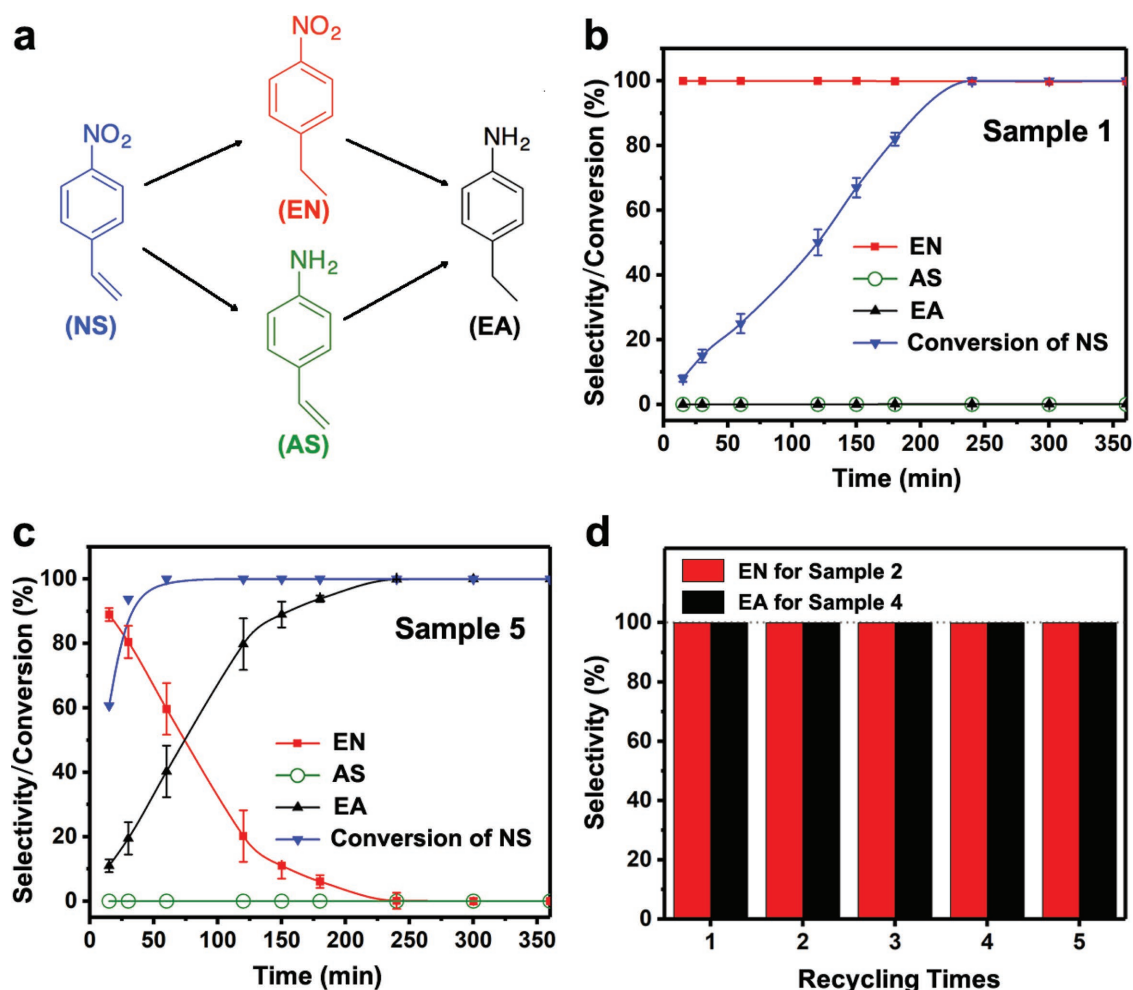


Figure 3. Catalytic performance of the hetero-phase Pd nanosheets with different crystallinities. a) Hydrogenation reaction of NS. b,c) Time-dependent catalysis in the hydrogenation of NS by using Samples 1 and 5, respectively, as the catalyst. Reaction conditions: room temperature, H₂ balloon. d) Recycling tests of Samples 2 and 4 in the hydrogenation of NS. Reaction conditions: room temperature, H₂ balloon, 150 min (2.5 h) for Sample 2, 60 min (1 h) for Sample 4.

hydrogenated product is 4-ethylbenzenamine (EA). Gas chromatography (GC) was adopted to track the reaction process, and the products were determined by GC-mass spectrometry (GC-MS) and nuclear magnetic resonance spectroscopy. The hydrogenation reaction was conducted at room temperature under H₂ atmosphere (see the Supporting Information for details). The time-dependent catalytic curves for the hydrogenation of NS by Samples 1 and 5 are shown in Figure 3b,c, respectively, in which, the conversion curve (blue) describes the percentage of NS converted to the products, whereas the selectivity curve (red, black or green) describes the molar ratio of the corresponding product (EN, EA, or AS) in the total products.

Based on our experimental results, it was found that Sample 1 possessed the high selectivity (>99%) toward the generation of EN throughout the reaction (Figure 3b), and a 100% conversion of NS was achieved after 240 min (4 h) of hydrogenation (Figures S3–S5, Supporting Information). The excellent selectivity toward EN (>99%) did not decrease even after hydrogenation for 30 h (Figure S6, Supporting Information), meaning that EN cannot be converted to the fully hydrogenated product (EA) by using Sample 1 as the catalyst. In comparison, in the hydrogenation reaction catalyzed by Sample 5, i.e., the

Pd nanosheets with the highest crystallinity among Samples 1–5, EN was the main product at the initial stage. With the prolonged hydrogenation reaction, EN was gradually converted to the fully hydrogenated product EA. After hydrogenation for 240 min (4 h), EA was the only product with a high purity over 99% (Figure S7, Supporting Information).

Besides the chemoselectivity, the catalytic activity is also dependent on the crystallinity of the hetero-phase Pd nanosheets. Compared with Sample 1, Sample 2 also exhibits high chemoselectivity (>99%) of EN, but its catalytic activity is higher than Sample 1. It only takes 150 min (2.5 h) to achieve the 100% conversion of NS (Figure S8, Supporting Information). To the best of our knowledge, Sample 2 is the best heterogeneous catalyst to hydrogenate the C=C double bond under mild conditions with high catalytic selectivity (>99%) and 100% conversion (Table S1, Supporting Information). Comparing the time-dependent catalytic curves of Samples 3–5 (Figure S9 and S10, Supporting Information and Figure 3c), all of the catalysts produce the fully hydrogenated product, i.e., EA. Among them, Sample 4 shows the highest catalytic activity, which completely converted NS to the fully hydrogenated product (EA) with a purity of >99% in 60 min (1 h, Figure S10, Supporting Information). Moreover,

Samples 2 and 4 also exhibited good stability. The catalytic selectivity did not decrease after recycling for five times (Figure 3d).

The time-dependent catalytic curves of Samples 1–5 (Figure 3b,c, Figures S8–S10, Supporting Information) show that the amorphous-dominant samples (Samples 1 and 2) exhibit higher chemoselectivity toward the hydrogenation of C=C double bonds and lower catalytic activity, compared with the crystalline-dominant samples (Samples 3–5). The possible reasons can be explained as follows. 1) Sample 1 presents a higher binding energy than Sample 5 (Figure 2j–l), indicating the electron density around Pd atoms in amorphous phase is lower than that in crystalline phase. It suggests the weaker Pd–Pd metallic bonds in amorphous phase, leading to a lower surface energy.^[13] Therefore, the amorphous Pd surface would preferentially adsorb and hydrogenate the groups with lower polarity, i.e., C=C bonds, but impede the hydrogenation of the functional groups with higher polarity, i.e., nitro groups, resulting in the excellent chemoselectivity in the amorphous-dominant samples (Samples 1 and 2). 2) The lower electron density around Pd atoms in the amorphous-dominant samples (Samples 1 and 2), which could result in a stronger surface binding with H atoms, and thus reduce the hydrogenation activity.^[14] 3) Although the same ligand is used during our synthesis in order to eliminate the ligand effect in catalysis, the different atomic arrangement in different phases indicates the different coordination environment at the ligand/metal interface,^[15] which may affect the catalytic activity and selectivity.^[16] However, there is still no effective technique to directly characterize the detailed surface and interface structures of metal nanomaterials.^[16a]

In summary, we report a one-pot wet-chemical method for the synthesis of amorphous/crystalline hetero-phase Pd nanosheets. The crystallinity of these nanosheets can be easily tuned by simply changing the reaction temperature. These nanosheets are used as the heterogeneous catalysts to study the chemoselectivity in hydrogenation of 4-nitrostyrene. It is found that the crystallinities of amorphous/crystalline hetero-phase Pd nanosheets play a critical role in the catalytic activity and chemoselectivity in the 4-nitrostyrene hydrogenation. The Pd nanosheets with high percentage of amorphous phase exhibit an excellent chemoselectivity, while those with high percentage of crystalline phase show a higher catalytic activity. This work not only presents a novel synthetic method for hetero-phase nanomaterials, but also provides a new strategy in controlling the catalytic activity and selectivity for fine chemical industries. We believe that more unique properties and promising applications in catalysis, optics, electronics, magnetism, mechanics, photothermal therapy, etc. will be discovered based on the synthesis of novel hetero-phase nanomaterials.

Supporting Information

Supporting Information is available from the Wiley Online Library or from the author.

Acknowledgements

N.Y. and H.C. contributed equally to this work. This work was supported by MOE under AcRF Tier 2 (ARC 19/15, Nos. MOE2014-T2-2-093; MOE2015-T2-2-057; MOE2016-T2-2-103; MOE2017-T2-1-162) and

AcRF Tier 1 (2016-T1-001-147; 2016-T1-002-051; 2017-T1-001-150; 2017-T1-002-119), and NTU under Start-Up Grant (M4081296.070.500000). The authors would like to acknowledge the Facility for Analysis, Characterization, Testing, and Simulation, Nanyang Technological University, Singapore, for their electron microscopy (and/or X-ray) facilities.

Conflict of Interest

The authors declare no conflict of interest.

Keywords

amorphous, catalysts, chemoselective, hetero-phase, Pd nanosheets

Received: May 21, 2018

Revised: June 29, 2018

Published online:

- [1] a) Y. Xia, Y. Xiong, B. Lim, S. E. Skrabalak, *Angew. Chem., Int. Ed.* **2009**, *48*, 60; b) H. Zhang, M. Jin, Y. Xia, *Angew. Chem., Int. Ed.* **2012**, *51*, 7656; c) H. Zhang, *ACS Nano* **2015**, *9*, 9451; d) Z. Fan, H. Zhang, *Chem. Soc. Rev.* **2016**, *45*, 63.
- [2] C. Tan, J. Chen, X.-J. Wu, H. Zhang, *Nat. Rev. Mater.* **2018**, *3*, 17089.
- [3] a) Y. Chen, Z. Fan, Z. Luo, X. Liu, Z. Lai, B. Li, Y. Zong, L. Gu, H. Zhang, *Adv. Mater.* **2017**, *29*, 1701331; b) Q. Lu, A.-L. Wang, Y. Gong, W. Hao, H. Cheng, J. Chen, B. Li, N. Yang, W. Niu, J. Wang, Y. Yu, X. Zhang, Y. Chen, Z. Fan, X.-J. Wu, J. Chen, J. Luo, S. Li, L. Gu, H. Zhang, *Nat. Chem.* **2018**, *10*, 456.
- [4] a) M.-P. Pileni, *Acc. Chem. Res.* **2017**, *50*, 1946; b) K. C. Poon, D. Tan, T. Vo, B. Khezri, H. Su, R. Webster, H. Sato, *J. Am. Chem. Soc.* **2014**, *136*, 5217.
- [5] M. R. Knecht, T. R. Walsh, *Bio-Inspired Nanotechnology—From Surface Analysis To Applications*, 1st ed., Springer-Verlag, New York **2014**, p. 143.
- [6] Y. Zhang, X. Zhu, J. Guo, X. Huang, *ACS Appl. Mater. Interfaces* **2016**, *8*, 20642.
- [7] X. Huang, S. Li, Y. Huang, S. Wu, X. Zhou, S. Li, C. L. Gan, F. Boey, C. A. Mirkin, H. Zhang, *Nat. Commun.* **2011**, *2*, 292.
- [8] a) E. V. Dubrovina, J. W. Gerritsen, J. Zivkovic, I. V. Yaminsky, S. Spellera, *Colloids Surf., B* **2010**, *76*, 63; b) J. C. Love, L. A. Estroff, J. K. Kriebel, R. G. Nuzzo, G. M. Whitesides, *Chem. Rev.* **2005**, *105*, 1103.
- [9] D.-G. Tong, W. Chu, Y.-Y. Luo, X.-Y. Ji, Y. He, *J. Mol. Catal. A: Chem.* **2007**, *265*, 195.
- [10] a) A. Corma, P. Serna, *Science* **2006**, *313*, 332; b) S. Furukawa, K. Takahashi, T. Komatsu, *Chem. Sci.* **2016**, *7*, 4476; c) G. Xu, H. Wei, Y. Ren, J. Yin, A. Wang, T. Zhang, *Green Chem.* **2016**, *18*, 1332; d) S. Furukawa, Y. Yoshida, T. Komatsu, *ACS Catal.* **2014**, *4*, 1441.
- [11] M. J. Beier, J.-M. Andanson, A. Baiker, *ACS Catal.* **2012**, *2*, 2587.
- [12] a) M. Makosch, W. Lin, V. Bumbálek, J. Sá, J. Medlin, K. Hungerbühler, J. van Bokhoven, *ACS Catal.* **2012**, *2*, 2079; b) K.-i. Shimizu, Y. Miyamoto, A. Satsuma, *J. Catal.* **2010**, *270*, 86.
- [13] J. G. Eberhart, S. Horner, *J. Chem. Educ.* **2010**, *87*, 608.
- [14] M. Zhao, K. Yuan, Y. Wang, G. Li, J. Guo, L. Gu, W. Hu, H. Zhao, Z. Tang, *Nature* **2016**, *539*, 76.
- [15] a) Y. Liu, C. Wang, Y. Wei, L. Zhu, D. Li, J. S. Jiang, N. M. Markovic, V. R. Stamenkovic, S. Sun, *Nano Lett.* **2011**, *11*, 1614; b) J. C. Love, L. A. Estroff, J. K. Kriebel, R. G. Nuzzo, G. M. Whitesides, *Chem. Rev.* **2005**, *105*, 1103.
- [16] a) P. Liu, R. Qin, G. Fu, N. Zheng, *J. Am. Chem. Soc.* **2017**, *139*, 2122; b) X. Zhao, L. Zhou, W. Zhang, C. Hu, L. Dai, L. Ren, B. Wu, G. Fu, N. Zheng, *Chem* **2018**, *4*, 1.